# Atomic Collision Processes for Astrophysical and Laboratory Plasmas

**M. S. PINDZOLA[1], S. D. LOCH[1], SH. A. ABDEL-NABY[1,2], T. G. LEE[1]**
**J. COLGAN[3], N. R. BADNELL[4] AND M. G. O'MULLANE[4]**

[1]*Department of Physics, Auburn University, Auburn, AL 36849, USA*
[2]*Department of Physics, BeniSuef University, BeniSuef, Egypt*
[3]*Theoretical Division, Los Alamos National Laboratory, Los Alamos, New Mexico 87545, USA*
[4]*University of Strathclyde, Glasgow, UK*
*E-mail: pindzola@physics.auburn.edu*

**ABSTRACT:** An accurate knowledge of atomic collision processes is important for a better understanding of many astrophysical and laboratory plasmas. First stage collision databases which contain electron-impact excitation, ionization, and recombination cross sections and temperature dependent rate coefficients have been constructed using perturbative distorted-wave methods and non-perturbative R-matrix pseudo-states and time-dependent close-coupling methods. Second stage collision databases which contain generalized collisional-radiative ionization, recombination, and power loss coefficients as a function of both temperature and density have also been constructed. We review the first and second stage methods and present recent atomic collision results and a guide to existing databases.

## 1. INTRODUCTION

Accurate atomic and molecular databases underpin current research efforts in a variety of scientific and engineering areas: including controlled fusion energy, astrophysics, radiation biophysics, fluorescent lamps, and atmospheric pollutant removal. For example, all light elements (H-O) are of interest for fusion experiments; in particular Li and B as wall coating materials and Be and C as primary wall materials.

Over the years both theory and experiment have provided increasingly more accurate cross sections for the electron-impact excitation, ionization, and recombination of atoms and their ions. In this paper we review perturbative distorted-wave methods and non-perturbative R-matrix with pseudo-states and time-dependent close-coupling methods in both their non-relativistic and fully-relativistic versions. Theory has also provided increasingly more accurate generalized collisional-radiative rate coefficients for electron-impact ionization, recombination, and power loss for atomic isonuclear sequences.

The rest of the review paper is structured as follows: in Section II we describe distorted-wave, R-matrix, and time-dependent close-coupling methods and give electron-impact ionization cross section examples, in Section III we describe first and second stage collisional databases and give a generalized collisional-radiative ionization rate coefficient example, while in Section IV we give a brief review of current projects.

## 2. BASIC COLLISION THEORY

### 2.1. Configuration-Average Distorted-Wave (CADW) Method

For electron-impact ionization a general transition between configurations has the form:

$$(n_0 l_0)^{\omega_0} k_i l_i \rightarrow (n_0 l_0)^{\omega_0 - 1} k_e l_e k_f l_f \qquad (1)$$

where $\omega_0$ is a subshell occupation number, $n_0$ $l_0$ are quantum numbers of the bound electron, and $k_i$ $l_i$, $k_e$ $l_e$, are quantum numbers of the initial, ejected, and final continuum electrons. The configuration-average ionization cross section is given by [1]:

$$\sigma_{ion} = \frac{32\,\omega_0}{k_i^3} \int_0^{E/2} \frac{d\epsilon_e}{k_e k_f} \sum_{l_i, l_e, l_f} (2l_i + 1)$$
$$\times (2l_e + 1)(2l_f + 1) S(n_0 l_0 k_i l_i \rightarrow k_e l_e k_f l_f), \tag{2}$$

where $k = \sqrt{2\epsilon}$ and the continuum normalization is one times a sine function. For electron-impact excitation a general transition between configurations has the form:

$$(n_1 l_1)^{\omega_1 + 1} (n_2 l_2)^{\omega_2 - 1} k_i l_i \rightarrow (n_1 l_1)^{\omega_1} (n_2 l_2)^{\omega_2} k_f l_f, \tag{3}$$

where $\omega_1$ and $\omega_2$ are subshell occupation numbers, $n_1 l_1$ and $n_2 l_2$ are quantum numbers of the bound electrons, and $k_i l_i$ and $k_f l_f$ are quantum numbers of the initial and final continuum electrons. The configuration-average excitation cross section is given by:

$$\sigma_{exc} = \frac{8\pi}{k_i^3 k_f} (\omega_1 + 1)(4l_2 + 3 - \omega_2)$$
$$\times \Sigma_{l_i, l_f} (2l_i + 1)(2l_f + 1) S(n_1 l_1 k_i l_i \rightarrow k_2 l_2 k_f l_f). \tag{4}$$
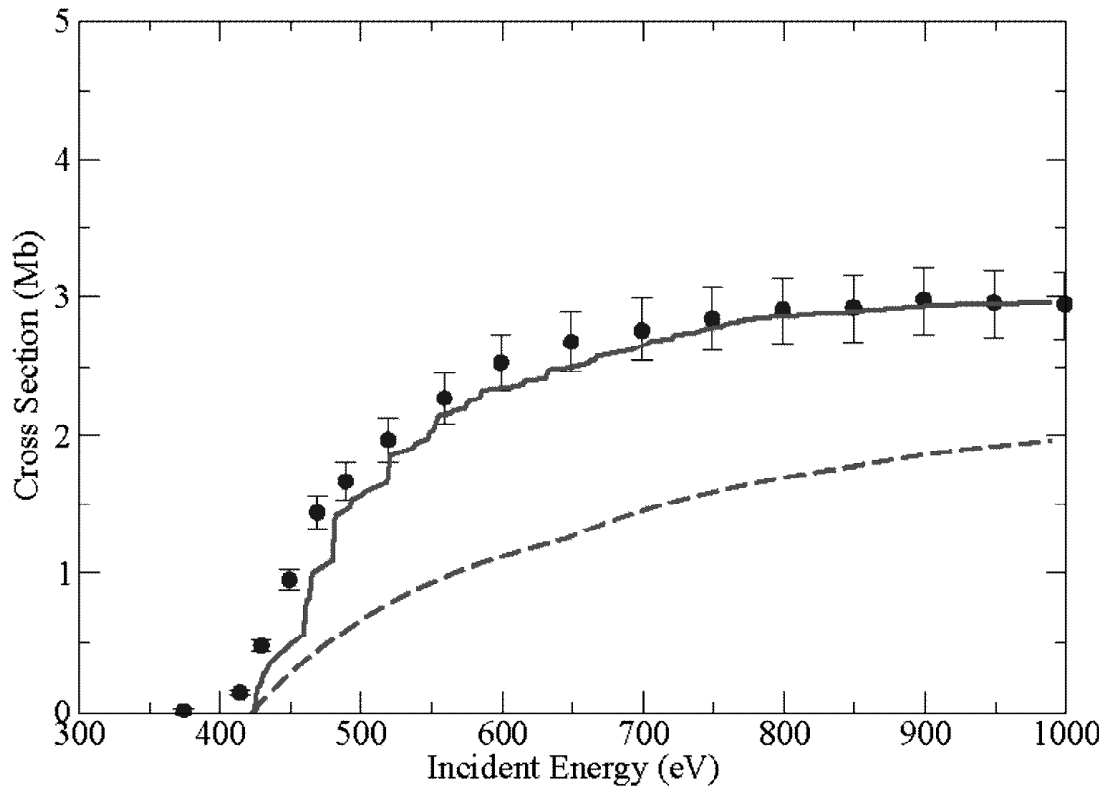


**Figure 1: Electron-impact ionization of W$^{17+}$. Solid line (red): CADW total ionization, dashed line (red): CADW direct ionization, circles (blue) with error bars:experiment [2] (1.0 Mb = 1.0 × 10$^{-18}$ cm$^2$).**

As an example, we calculated the electron-impact ionization of $W^{17+}$ and compared with experiment [2] in Figure 1. Direct ionization cross sections were included using Eq.(2) for the *4f, 4d,* and *4p* subshells. Excitation-autoionization cross sections were included using Eq. (4) for those $4d \to nl, 4p \to nl$, , and $4s \to nl$ excitations which have energy thresholds above the ionization potential of the *4f* subshell. Good agreement is found between the CADW calculations and experiment.

For dense plasmas the initial and final distorted-waves and the Coulomb matrix elements found in $S(n_0 l_0 k_i l_i \to k_e l_e k_f l_f)$ of Eq. (2) and $S(n_1 l_1 k_i l_i \to k_2 l_2 k_f l_f)$ of Eq. (4) are modified to include an exponential screening factor:

$$SF(r) = e^{-r/\Lambda}, \tag{5}$$

where the Debye-Huckel screening radius $\Lambda = \sqrt{T_e / 4\pi N_e}$, $T_e$ is the electron temperature, and $N_e$ is the electron density.

As an example, we calculated [3] the electron-impact ionization of the *2p* subshell of $Ne^{4+}$ for $T_e = 500$ eV and various $N_e$ as shown in Figure 2. The ionization cross section peak drops as the electron density becomes larger.
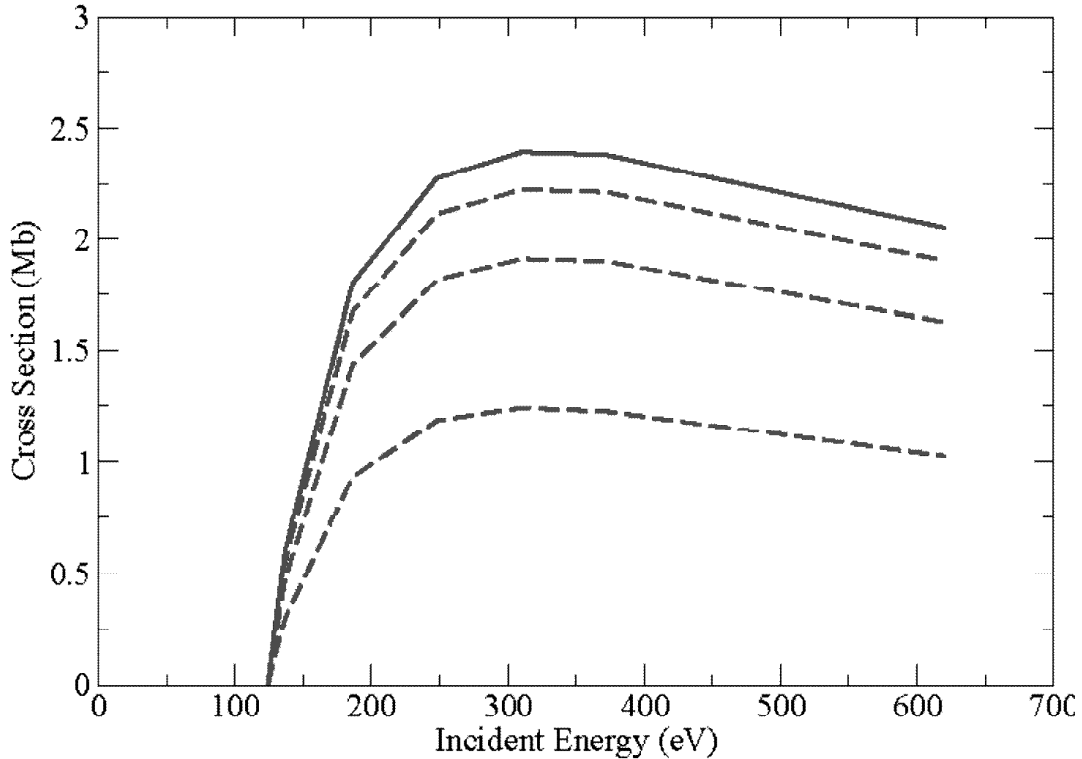


**Figure 2: Electron-impact ionization of $Ne^{4+}$. Solid line (red): CADW total ionization, upper dashed line (red): CADW direct ionization for $N_e = 10^{22}$ cm$^{-3}$, middle dashed line (red): CADW direct ionization for $N_e = 10^{23}$ cm$^{-3}$, lower dashed line (red): CADW direct ionization for $N_e = 10^{24}$ cm$^{-3}$ (1.0 Mb = 1.0 × 10$^{-18}$ cm$^2$).**

## 2.2. Sub-Configuration-Average Distorted-Wave (SCADW) Method

For electron-impact ionization a general transition between sub-configurations has the form:

$$(n_0 l_0 j_0)^{\omega_0} p_i l_i j_i \to (n_0 l_0 j_0)^{\omega_0 - 1} p_e l_e j_e p_f l_f j_f, \tag{6}$$

where $\omega_0$ is a subshell occupation number, $n_0 l_0 j_0$ are quantum numbers of the bound electron, and $p_i l_i j_i, p_e l_e j_e$ and $p_f l_f j_f$ are quantum numbers of the initial, ejected, and final continuum electrons. The subconfiguration-average ionization cross section is given by[4]:

$$\sigma_{ion} = \frac{16\omega_0}{p_i^3} \int_0^{E/2} \frac{d\epsilon_e}{p_e p_f} \sum_{l_i,l_e,l_f} \sum_{j_i,j_e,j_f} (2j_i+1)$$

$$\times (2j_e+1)(2j_f+1)S(n_0 l_0 j_0 p_i l_i j_i \rightarrow p_e l_e j_e p_f l_f j_f), \quad (7)$$

where $p = \sqrt{2\epsilon + \epsilon^2/c^2}$ and the continuum normalization is $\sqrt{1+\epsilon/c^2}$ times a sine function.

For electron-impact excitation a general transition between subconfigurations has the form:

$$(n_1 l_1 j_1)^{\omega_1+1} (n_2 l_2 j_2)^{\omega_2-1} p_i l_i j_i \rightarrow (n_1 l_1 j_1)^{\omega_1} (n_2 l_2 j_2)^{\omega_2} p_f l_f j_f, \quad (8)$$

where $\omega_1$ and $\omega_2$ are subshell occupation numbers, $n_1 l_1 j_1$ and $n_2 l_2 j_2$ are quantum numbers of the bound electron, and $p_i l_i j_i$ and $p_f l_f j_f$ are quantum numbers of the initial and final electrons. The subconfiguration-average excitation cross section is given by:

$$\sigma_{exc} = \frac{8\pi}{p_i^3 p_f}(\omega_1+1)(4j_2+2-\omega_2)$$

$$\times \Sigma_{l_i,l_f} \Sigma_{j_i,j_f} (2j_i+1)(2j_f+1) S(n_1 l_1 j_1 p_i l_i j_1 \rightarrow n_2 l_2 j_2 p_f l_f j_f). \quad (9)$$
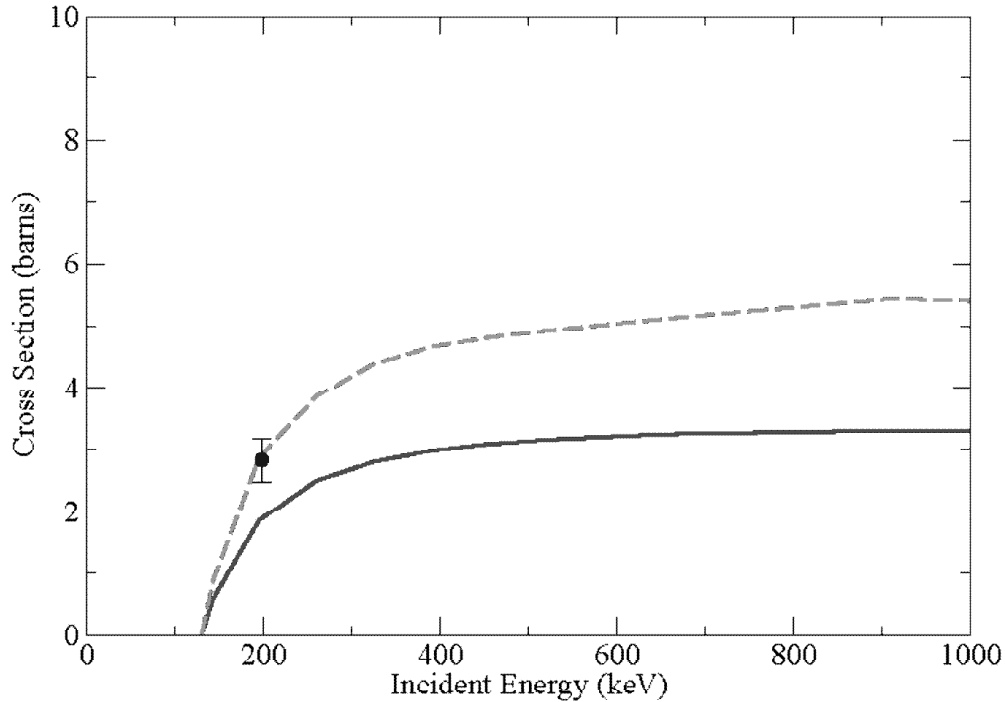


**Figure 3: Electron-impact ionization of U[90+]. Solid line (red): SCADW electrostatic, dashed line (green): SCADW retarded electromagnetic, circle (blue) with error bar: experiment [6] (1.0 b = 1.0 × 10^{-24} cm²)**

As a first example, we calculated[5] the electron-impact ionization of U[90+] and compared with experiment[6] in Figure 3. Direct ionization cross sections were made using Eq. (7) with the scattering probabilities, $S(n_0 l_0 j_0 p_i l_i j_i \rightarrow p_e l_e j_e p_f l_f j_f)$, calculated including only the electrostatic interaction and including the full retarded electromagnetic interaction. The SCADW retarded electromagnetic cross sections are in good agreement with experiment at 198 keV. We also calculated[5] the electron-impact ionization of the M2 subshell of U and compared with experiment[7] in Figure 4. Both the SCADW electrostatic and SCADW retarded electromagnetic cross sections are in good agreement with experiment.

## 2.3. R-Matrix Pseudo-States (RMPS) Method

The R-Matrix method [8] splits the scattering process into two regions. The total wavefunction in the inner region is given by:
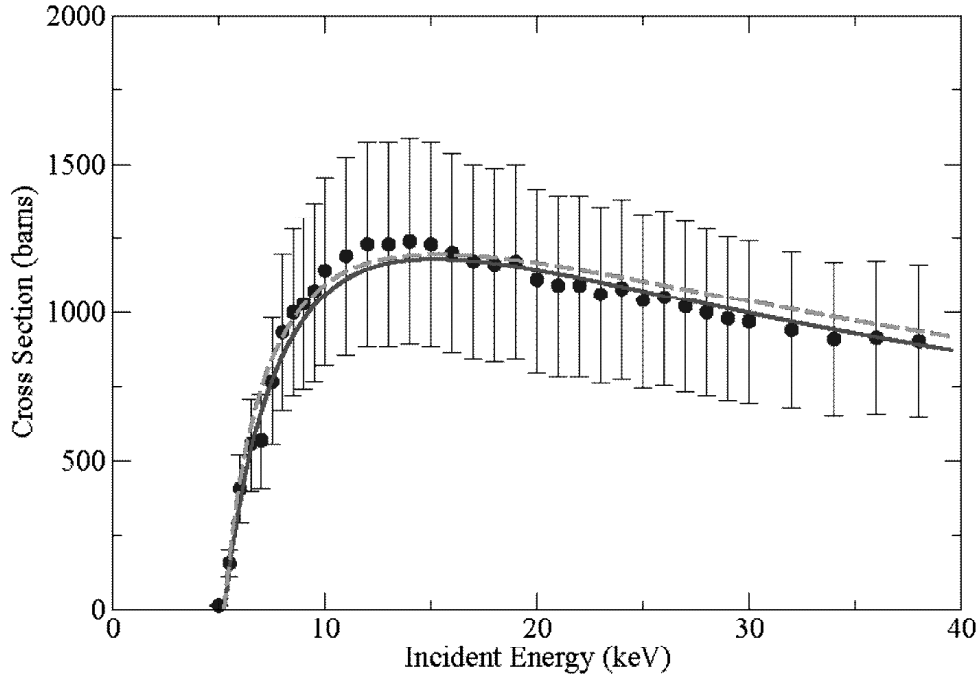


**Figure 4: Electron-impact ionization of the M2 subshell of Uranium. Solid line (red):SCADW electrostatic, dashed line (green): SCADW retarded electromagnetic, circles (blue) with error bars: experiment [7] (1.0 b = 1.0 × 10⁻²⁴ cm²).**

$$\Psi_k^{N+1} = A\, \Sigma_{i,j}\, a_{ijk}\, \psi_i^{N+1} \frac{u_{ij}(r_{N+1})}{r_{N+1}} + \Sigma_i b_{ik} \chi_i^{N+1}, \tag{10}$$

where $A$ is an antisymmetrization operator, $\psi_i^{N+1}$ are channel functions obtained by coupling $N$- electron target states with the angular and spin functions of the scattered electron, $u_{ij}(r)$ are radial continuum basis functions, and $\chi_i^{N+1}$ are bound functions which ensure the completeness of the total wavefunction. The coefficients $a_{ijk}$ and $b_{ik}$ are determined by diagonalization of the total ($N+1$) electron Hamiltonian. The total wavefunction in the outer region is given by:

$$\Psi_k^{N+1} = \Sigma_i \psi_i^{N+1} \frac{v_i(r_{N+1})}{r_{N+1}}, \tag{11}$$

where the radial wavefunctions $v_i(r)$ are obtained by solving the coupled differential equations given by:

$$[T_i(r) + V_{ij}(r)]\, v_i(r) = 0 \tag{12}$$

where $T_i(r)$ is a kinetic and nuclear energy operator and $V_{ij}(r)$ is an asymptotic coupling operator. The inner and outer region solutions are matched at the boundary and the K-matrix is extracted. Excitation cross sections are obtained by relating the K-matrix to the S-matrix.

Over the years, a non-relativistic RMLS suite of codes has been developed for

low Z atoms and ions, a semi-relativistic RMLSJ suite of codes has been developed for medium Z atoms and ions, and a fully-relativistic RMjjJ suite of codes has been developed for high Z atoms and ions. With the addition of pseudo-states, the R-matrix method becomes more accurate for excitation to high-lying excited states. The RMPS method can also be used to calculate electron-impact ionization cross sections, including both direct ionization and excitation-autoionization.

## 2.4. Time-Dependent Close-Coupling (TDCC) Method

The time-dependent Schrodinger equation for two-active electron atomic systems is given by:

$$i\frac{d\,\Psi(\vec{r}_1,\vec{r}_2,t)}{dt} = H(\vec{r}_1,\vec{r}_2)\Psi(\vec{r}_1,\vec{r}_2,t), \tag{13}$$

where

$$H(\vec{r}_1,\vec{r}_2) = -\frac{1}{2}\nabla_1^2 + V(r_1) - \frac{1}{2}\nabla_2^2 + V(r_2) + \frac{1}{|\vec{r}_1 - \vec{r}_2|}. \tag{14}$$

Expanding in coupled spherical harmonics:

$$\Psi(\vec{r}_2,\vec{r}_2,t) = \Sigma_{l_2,l_2}\frac{P_{l_1 l_2}^{LS}(r_1,r_2,t)}{r_1 r_2}\Sigma_{m_1,m_2}\,C_{m_1 m_2 M}^{l_1 l_2 L}\,Y_{l_1 m_1}(\hat{r}_1)Y_{l_2 m_2}(\hat{r}_2) \tag{15}$$

yields the time-dependent close-coupled equations [9]:

$$i\frac{dP_{l_1 l_2}^{LS}(r_1,r_2,t)}{dt} = [T_{l_1}(r_1) + T_{l_2}(r_2)]P_{l_1 l_2}^{LS}(r_1,r_2,t)$$

$$+ \Sigma_{l_1',l_2'}V_{l_1 l_2,l_1' l_2'}^{L}(r_1,r_2,t)\,P_{l_1' l_2'}^{LS}(r_1,r_2,t) \tag{16}$$

where

$$T_l(r) = -\frac{1}{2}\frac{\partial^2}{\partial r^2} + \frac{l(l+1)}{2r^2} + V(r) \tag{17}$$

and $V_{l_1 l_2,l_1' l_2'}^{L}(r_1,r_2,t)$ is a two-body coupling operator.

The time-dependent Dirac equation for two-active electron atomic systems is given by:

$$i\frac{d\,\vec{\Psi}(\vec{r}_1,\vec{r}_2,t)}{dt} = H(\vec{r}_1,\vec{r}_2)\,\Psi(\vec{r}_1,\vec{r}_2,t), \tag{18}$$

$$H(\vec{r}_1,\vec{r}_2) = \begin{pmatrix} V(\vec{r}_1,\vec{r}_2) & c\,\vec{\sigma}.\vec{p}_1 & c\,\vec{\sigma}.\vec{p}_2 & 0 \\ c\,\vec{\sigma}.\vec{p}_1 & V(\vec{r}_1,\vec{r}_2) - 2c^2 & 0 & c\,\vec{\sigma}.\vec{p}_2 \\ \vec{\sigma}.\vec{p}_2 & 0 & V(\vec{r}_1,\vec{r}_2) - 2c^2 & c\,\vec{\sigma}.\vec{p}_1 \\ 0 & c\,\vec{\sigma}.\vec{p}_2 & c\,\vec{\sigma}.\vec{p}_1 & V(\vec{r}_1,\vec{r}_2) - 4c^2 \end{pmatrix} \tag{19}$$

Expanding in coupled spin-orbit eigenfunctions:

$$\vec{\Psi}(\vec{r}_1,\vec{r}_2,t) =$$

$$
\begin{pmatrix}
\sum_{j_1 j_2} \dfrac{PP^J_{k_1 k_2}(r_1,r_2,t)}{r_1 r_2} \sum_{m_1 m_2} C^{j_1 j_2 J}_{m_1 m_2 M} \Phi_{+k_1,m_1}(\theta_1,\varphi_1)\Phi_{+k_2,m_2}(\theta_2,\varphi_2) \\[2ex]
i\sum_{j_1 j_2} \dfrac{QP^J_{k_1 k_2}(r_1,r_2,t)}{r_1 r_2} \sum_{m_1 m_2} C^{j_1 j_2 J}_{m_1 m_2 M} \Phi_{-k_1,m_1}(\theta_1,\varphi_1)\Phi_{+k_2,m_2}(\theta_2,\varphi_2) \\[2ex]
i\sum_{j_1 j_2} \dfrac{PQ^J_{k_1 k_2}(r_1,r_2,t)}{r_1 r_2} \sum_{m_1 m_2} C^{j_1 j_2 J}_{m_1 m_2 M} \Phi_{+k_1,m_1}(\theta_1,\varphi_1)\Phi_{-k_2,m_2}(\theta_2,\varphi_2) \\[2ex]
\sum_{j_1 j_2} \dfrac{QQ^J_{k_1 k_2}(r_1,r_2,t)}{r_1 r_2} \sum_{m_1 m_2} C^{j_1 j_2 J}_{m_1 m_2 M} \Phi_{-k_1,m_1}(\theta_1,\varphi_1)\Phi_{-k_2,m_2}(\theta_2,\varphi_2)
\end{pmatrix}
\tag{20}
$$

yields the time-dependent close-coupled equations[10]:

$$
\begin{aligned}
i\frac{\partial PP^J_{k_1 k_2}(r_1,r_2,t)}{\partial t} =\ & [V(r_1)+V(r_2)]PP^J_{k_1 k_2}(r_1,r_2,t) \\
& + \sum_{k_1',k_2'} W^J_{+k_1,+k_2,+k_1',+k_2'}(r_1,r_2,t)\, PP^J_{k_1' k_2'}(r_1,r_2,t) \\
& - c\left(\frac{\partial}{\partial r_1}-\frac{k_1}{r_1}\right)QP^J_{k_1 k_2}(r_1,r_2,t) - c\left(\frac{\partial}{\partial r_2}-\frac{k_2}{r_2}\right)PQ^J_{k_1 k_2}(r_1,r_2,t),
\end{aligned}
\tag{21}
$$

$$
\begin{aligned}
i\frac{\partial QP^J_{k_1 k_2}(r_1,r_2,t)}{\partial t} =\ & [V(r_1)+V(r_2)-2c^2]QP^J_{k_1 k_2}(r_1,r_2,t) \\
& + \sum_{k_1',k_2'} W^J_{-k_1,+k_2,-k_1',+k_2'}(r_1,r_2,t)\, QP^J_{k_1' k_2'}(r_1,r_2,t) \\
& + c\left(\frac{\partial}{\partial r_1}+\frac{k_1}{r_1}\right)PP^J_{k_1 k_2}(r_1,r_2,t) + c\left(\frac{\partial}{\partial r_2}-\frac{k_2}{r_2}\right)QQ^J_{k_1 k_2}(r_1,r_2,t),
\end{aligned}
\tag{22}
$$

$$
\begin{aligned}
i\frac{\partial PQ^J_{k_1 k_2}(r_1,r_2,t)}{\partial t} =\ & [V(r_1)+V(r_2)-2c^2]PQ^J_{k_1 k_2}(r_1,r_2,t) \\
& + \sum_{k_1',k_2'} W^J_{+k_1,-k_2,+k_1',-k_2'}(r_1,r_2,t)\, PQ^J_{k_1' k_2'}(r_1,r_2,t) \\
& + c\left(\frac{\partial}{\partial r_1}-\frac{k_1}{r_1}\right)QQ^J_{k_1 k_2}(r_1,r_2,t) + c\left(\frac{\partial}{\partial r_2}+\frac{k_2}{r_2}\right)QQ^J_{k_1 k_2}(r_1,r_2,t),
\end{aligned}
\tag{23}
$$

$$
\begin{aligned}
i\frac{\partial QQ^J_{k_1 k_2}(r_1,r_2,t)}{\partial t} =\ & [V(r_1)+V(r_2)-4c^2]QQ^J_{k_1 k_2}(r_1,r_2,t) \\
& + \sum_{k_1',k_2'} W^J_{-k_1,-k_2,+k_1',-k_2'}(r_1,r_2,t)\, QQ^J_{k_1' k_2'}(r_1,r_2,t) \\
& - c\left(\frac{\partial}{\partial r_1}+\frac{k_1}{r_1}\right)QP^J_{k_1 k_2}(r_1,r_2,t) - c\left(\frac{\partial}{\partial r_2}+\frac{k_2}{r_2}\right)PQ^J_{k_1 k_2}(r_1,r_2,t),
\end{aligned}
\tag{24}
$$

where $W^J_{k_1,k_2,k'_1,k'_2}(r_1, r_2)$ is a two-body coupling operator.

After time propagation of the non-relativistic or fully-relativistic TDCC equations, scattering probabilities and cross sections are obtained by projecting the $P^{LS}_{l_1 l_2}(r_1, r_2, t \to \infty)$ or $PP^J_{k_1 k_2}(r_1, r_2, t \to \infty)$ etc. radial wavefunctions onto antisymmetrized products of bound and continuum radial orbitals.

### 2.5. Comparison of the CADW, RMPS, and TDCC Methods

As an example, we calculated[11] the electron-impact ionization of Al and compared with experiment[12] in Figures 5-6. CADW direct ionization cross sections were included using Eq.(2) for the 3p and 3s subshells in Figure 5. CADW excitation-autoionization cross sections were included using Eq.(4) for the 3s → 3p, 3d and 3s → 4l(l = 0 – 3) excitations in Figure 5. The CADW total ionization cross section is about a factor of 2 above experiment. TDCC direct ionization cross sections were included for the 3p and 3s subshells in Figure 6. RMPS total ionization cross sections are also shown in Figure 6. Good agreement is found between the RMPS total ionization calculations and experiment.
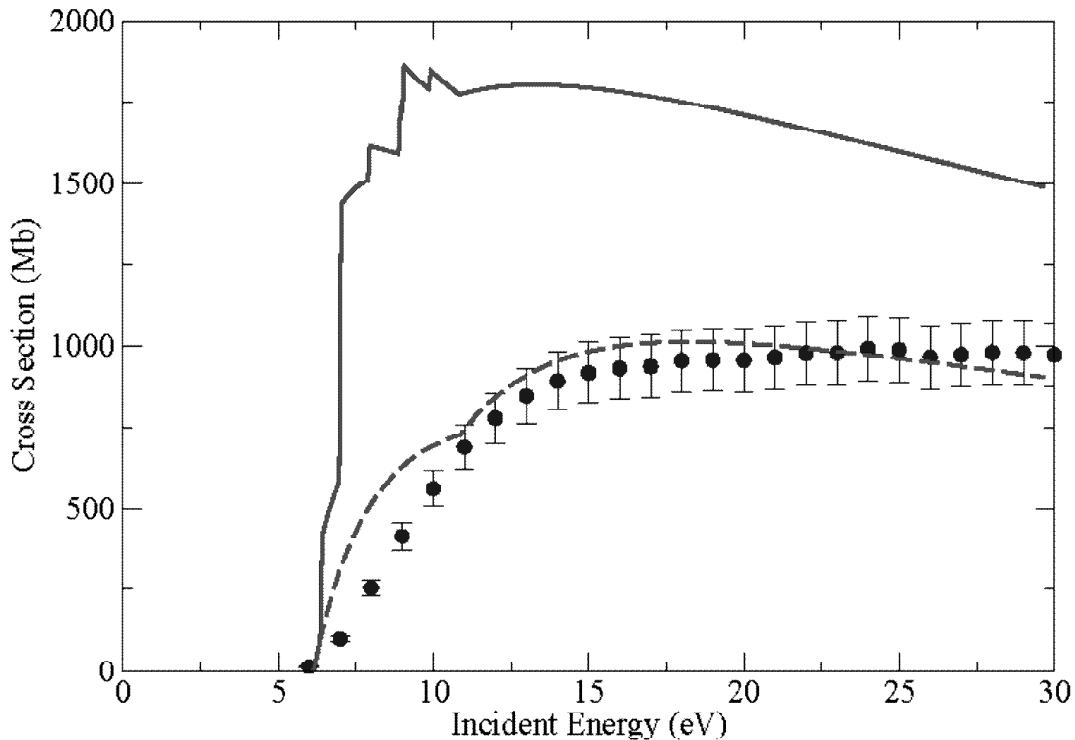


**Figure 5: Electron-impact ionization of Aluminum. Solid line (red): CADW total ionization, dashed line (red): CADW direct ionization, circles (blue) with error bars: experiment [12] (1.0 Mb = 1.0 × 10⁻¹⁸ cm²).**

## 3.  COLLISIONAL-RADIATIVE THEORY

### 3.1. First Stage Collision Database

Effective collision strengths (dimensionless) versus temperatures (in K) are stored in the first stage collision database. The effective collision strengths, obtained by Maxwellian convolution of the cross sections, are given by:

$$\Omega_{i \to f}(T_e) = \int_0^\infty \omega_i \frac{\epsilon_i}{I_H} \frac{\sigma_{i \to f}}{\pi a_0^2} e^{-\left(\frac{\epsilon_f}{kT_e}\right)} d\left(\frac{\epsilon_f}{kT_e}\right) \tag{25}$$

where $\omega_i$ is the statistical weight of the initial LS term, $\epsilon_i$ and $\epsilon_f$ are initial and final electron energies (in eV), $I_H = 13.6$ eV, $\sigma_{i \to f}$ is the excitation cross section (in cm$^2$), $kT_e$ is the temperature (in eV), and $a_0 = 5.29 \times 10^{-9}$cm. One can easily transform the stored effective collision strengths into excitation rate coefficients (in cm$^3$/sec) given by:

$$q_{i \to f}(T_e) = 2\sqrt{\pi}\, \alpha\, c\, a_0^2 \frac{1}{\epsilon_f} \frac{I_H}{kT_e} \Omega_{i \to f}(T_e) \tag{26}$$
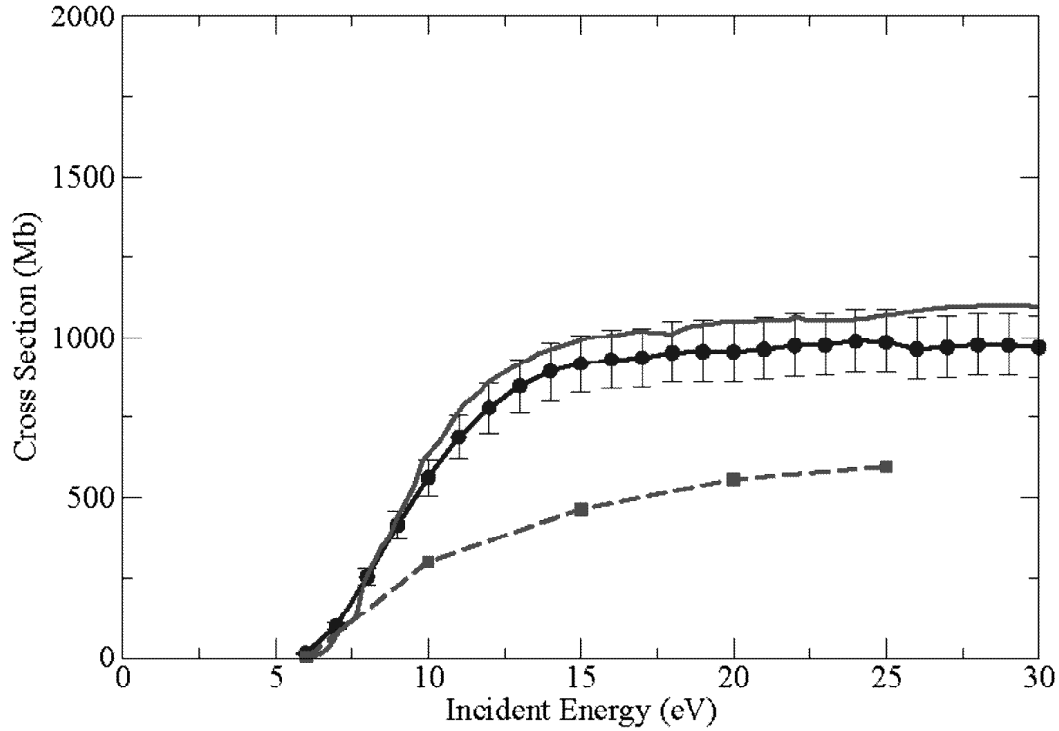


**Figure 6: Electron-impact ionization of Aluminum. Solid line (red): RMPS total ionization, dashed line (red): TDCC direct ionization, circles (blue) with error bars: experiment [12] (1.0 Mb = 1.0 × 10⁻¹⁸ cm²).**

where $\alpha = 1/137$ and $c = 3.0 \times 10^{10}$cm/sec. The effective collision strengths are stored since they do not vary as much with temperature as the rate coefficients.

Scaled ionization rate coefficients (in cm3/sec) versus temperatures (in K) are stored in the first stage collision database. The scaled ionization rate coefficients are given by:

$$\overline{s}_{i \to f}(T_e) = s_{i \to f}(T_e) e^{-\left(\frac{I_P}{kT_e}\right)}, \tag{27}$$

where $I_P$ is the ionization potential (in eV). Ionization rate coefficients are given by:

$$s_{i \to f}(T_e) = \frac{2\alpha c}{\sqrt{\pi}} \left(\frac{1}{I_H}\right)^{1/2} \left(\frac{1}{kT_e}\right)^{3/2} \int_{I_P}^{\infty} \epsilon_i\, \sigma_{i \to f} e^{-\left(\frac{\epsilon_i}{kT_e}\right)} d\epsilon_i, \tag{28}$$

where $\sigma_{i \to f}$ is the ionization cross section (in cm$^2$). The scaled ionization rate coefficients are stored since they do not vary as much with temperature as the rate coefficients.

Recombination rate coefficients (in cm3/sec) versus temperatures (in K) are stored in the first stage collision database. The recombination rate coefficients are given by:

$$r_{i \to f}(T_e) = \frac{2\alpha c}{\sqrt{\pi}}\left(\frac{1}{I_H}\right)^{1/2}\left(\frac{1}{kT_e}\right)^{3/2}\int_0^\infty r_{i \to f} \, {}^{-\left(\frac{\epsilon_i}{kT_e}\right)} d\epsilon_i, \tag{29}$$

where $\sigma_{i \to f}$ is the recombination cross section (in cm$^2$). The recombination rate coefficients generally vary smoothly with temperature.

## 3.2. Second Stage Collision Database

The first stage atomic collision data can be used directly to calculate term populations for all ground and excited states ($j, k$) via the basic collisional-radiative equations:

$$\frac{dN_j^z}{dt} = -\sum_{j'<j}\alpha_{j \to j'}N_j^z - N_e\sum_{j'\neq j}q_{j \to j'}N_j^z + \sum_{j'>j}a_{j' \to j}N_{j'}^z$$
$$+ N_e\Sigma_{j'\neq j}\,q_{j' \to j}N_{j'}^z - N_e\Sigma_k s_{j \to k}\,N_j^z + N_e\Sigma_k r_{k \to j}\,N_k^{z+1}, \tag{30}$$

where $\alpha_{j \to j'}$ are radiative decay rates, $q_{j \to j'}$ are electron-impact excitation rates, $s_{j \to k}$ are electron-impact ionization rates, $r_{k \to j}$ are electron-impact recombination rates, and $N_e$ is the electron density.

For many plasma conditions, the ground and metastable term populations evolve on a much slower timescale than the excited term populations, allowing the time derivative of the excited term populations to be set to zero. In the quasi-static equilibrium approximation, the term populations for all ground and metastable states ($\alpha, \beta, \gamma$) can be calculated via the generalized collisional-radiative (GCR) equations [13, 14]:

$$\frac{dN_\beta^z}{dt} = N_e\sum_{\beta'\neq\beta}(X_{\beta \to \beta'} + Q_{\beta \to \beta'})N_\beta^z + N_e\sum_{\beta'\neq\beta}(X_{\beta' \to \beta} + Q_{\beta' \to \beta})N_{\beta'}^z$$

$$-N_e\sum_\gamma S_{\beta \to \gamma}N_\beta^z + N_e\sum_\alpha S_{\alpha \to \beta}N_\alpha^{z-1}$$

$$+N_e\Sigma_\gamma R_{\gamma \to \beta}N_\gamma^{z+1} - N_e\Sigma_\alpha R_{\beta \to \alpha}N_\beta^z, \tag{31}$$

where $X_{\beta \to \beta'}$ and $Q_{\beta \to \beta'}$ are cross-coupling rate coefficients, $S_{\alpha \to \beta}$ are generalized ionization rate coefficients, and $R_{\beta \to \alpha}$ are generalized recombination rate coefficients. The generalized collisional-radiative coefficients are a function of both temperature and density. The generalized collisional-radiative coefficients are most useful in plasma transport studies, since they contain the effects of the excited states on the ground and metastables without the need for a large number of coefficients to be archived.

For example, the GCR ionization rate coefficient is given by:

$$S_{\beta \to \gamma} = s_{\beta \to \gamma} - \Sigma_{j'}\left(C_{jj'}^z\right)^{-1}C_{j'\beta}^z, \tag{32}$$

where $C_{jj'}^z$ are given in terms of $a_{j \to j'}$ and $q_{j \to j'}$. We present the GCR ionization rate coefficient at $T_e = 0.35$ eV for the $1\sigma^2 2\sigma$ $^2$S ground state of Li in Figure 7.

## 3.3. Isonuclear Sequence Databases

Over the last decade light atom isonuclear sequence first and second stage databases have been assembled based on the most accurate basic collision cross section calculations.
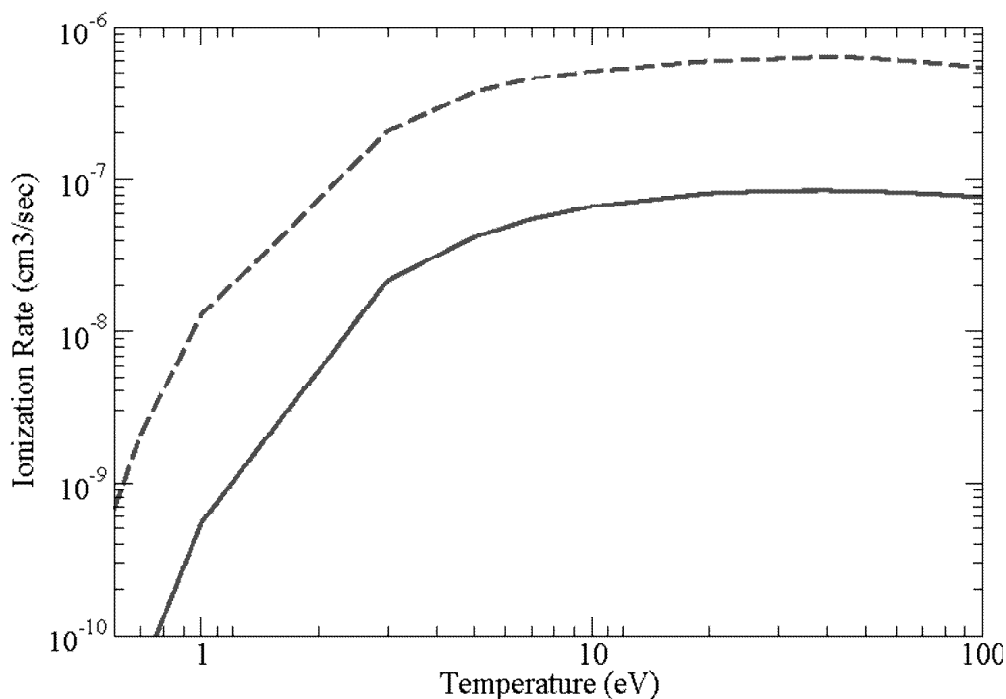
**Figure 7: GCR ionization rate coefficient for Lithium. Solid line (red): $N_e = 10^8 cm^{-3}$, dashed line (red): $N_e = 10^{14} cm^{-3}$.**

Accurate databases are now available for H[15], He[15], Li[16], Be[17], and B[18],while work is in progress for C, N, O, and Ne. Electronic data is available at IAEA/ALADDIN[19]. We also note that previous CADW calculations for the electron-impact ionization of the Fe[20], Ni[21], Kr[22], Sn[23], Xe[23], and W[24] isonuclear sequences are being updated with RMPS and TDCC calculations for the atoms and low-charged ions.

## 4. SUMMARY

We have reviewed the distorted-wave, R-matrix, and time-dependent close-coupling methods and showed calculations of ionization cross sections for various atoms and ions. We have also reviewed the generalized collisional-radiative method and showed a calculation of the ionization rate coefficient for the Li atom. We are currently generating accurate electron-impact excitation, ionization, and recombination cross sections for the N isonuclear sequence, while also generating accurate generalized collisional-radiative ionization, recombination, and power loss coefficients for the C isonuclear sequence. In the future we plan to calculate accurate electron-impact excitation and ionization cross sections for atoms and low-charged ions in the Mn, Fe, Co, and Ni isonuclear sequences, as well as in the heavier Mo, Xe, La, W, Au, and U isonuclear sequences.

### *References*

[1]  M. S. Pindzola, D. C. Griffin, and C. Bottcher, NATO Advanced Study Institute, *Series B: Physics,* **145**, 75 (1986).

[2]  J. Rausch, A. Becker, K. Spruck, J. Hellhund, A. Borovik Jr., K. Huber, S. Schippers, and A. Muller, *J. Phys. B* **44**, 165202 (2011).

[3]  M. S. Pindzola, S. D. Loch, J. Colgan, and C. J. Fontes, *Phys. Rev. A* 77, 062707 (2008).

[4]  M. S. Pindzola and M. J. Buie, *Phys. Rev. A* **37**, 3232 (1988).

[5]  M. S. Pindzola and C. P. Ballance, *Phys. Rev. A* (2014).

[6]   R. E. Marrs, S. R. Elliott, and D. A. Knapp, *Phys. Rev. Lett.* **72**, 4082 (1994).

[7]   A. Moy, C. Merlet, X. Liovet, and O. Dugne, *J. Phys. B* **47**, 055202 (2014).

[8]   P. G. Burke, *R-Matrix Theory of Atomic Collisions*, Springer Series on Atomic, Optical, and Plasma Physics **61** (2011).

[9]   M. S. Pindzola, F. Robicheaux, S. D. Loch, J. C. Berengut, T. Topcu, J. Colgan, M. Foster, D. C.Griffin, C. P. Ballance, D. R. Schultz, T. Minami, N. R. Badnell, M. C. Witthoeft, D. R. Plante,D. M. Mitnik, J. A. Ludlow, and U. Kleiman, *J. Phys. B* **40**, R39 (2007).

[10]  M. S. Pindzola, J. A. Ludlow, F. Robicheaux, J. Colgan, and C. J. Fontes, *Phys. Rev. A* **80**, 052706 (2009).

[11]  S. D. Loch, C. P. Ballance, D. Wu, S. A. Abdel-Naby, and M. S. Pindzola, *J. Phys. B* **46**, 065201 (2012).

[12]  R. S. Freund, R. C. Wetzel, J. S. Randy, and T. R. Hayes, Phys. Rev. A **41**, 3575, (1990).

[13]  H. P. Summers, N. R. Badnell, M. G. O'Mullane, A. D. Whiteford, R. Bingham, B. J. Kellett, J.Lang, K. H. Behringer, U. Fantz, K. D. Zastrow, S. D. Loch, M. S. Pindzola, D. C. Griffin, andC. P. Ballance, Plasma Phys. Control. Fusion **44**, B323 (2002).

[14]  ADAS User Manual, H. P. Summers (2001), *http://adas.phys.strath.ac.uk*

[15]  S. D. Loch, C. P. Ballance, M. S. Pindzola, and D. P. Stotler, Plasma Phys. *Control. Fusion* **51**, 105006 (2009).

[16]  S. D. Loch, J. Colgan, M. C. Witthoeft, M. S. Pindzola, C. P. Ballance, D. M. Mitnik, D. C. Griffin, M. G. O'Mullane, and H. P. Summers, ADNDT **92**, 813 (2006).

[17]  S. D. Loch, M. S. Pindzola, C. P. Ballance, D. C. Griffin, J. Colgan, N. R. Badnell, M. G. O'Mullane, and H. P. Summers, ADNDT **94**, 257 (2008).

[18]  S. D. Loch, C. P. Ballance, M. S. Pindzola, D. C. Griffin, J. Colgan, N. R. Badnell, and M. G. O'Mullane, *J. Phys. Conf. Ser.* (2013).

[19]  IAEA/ALADDIN *www-amdis.iaea.org/ALADDIN*.

[20]  M. S. Pindzola, D. C. Griffin, C. Bottcher, S. M. Younger, and H. T. Hunter, *Nucl. Fusion Suppl. Issue* **1**, 21 (1987).

[21]  M. S. Pindzola, D. C. Griffin, C. Bottcher, M. J. Buie, and D. C. Gregory,  PhysicaScripta T **37**,35 (1991).

[22]  S. D. Loch, M. S. Pindzola, C. P. Ballance, D. C. Griffin, D. M. Mitnik, N. R. Badnell, M. G.O'Mullane, H. P. Summers, and A. D. Whiteford, *Phys. Rev. A* **66**, 052708 (2002).

[23]  S. D. Loch, M. S. Pindzola, and D. C. Griffin, Int. J. Mass. Spec. **271**, 68 (2008).

[24]  S. D. Loch, J. A. Ludlow, M. S. Pindzola, A. D. Whiteford, and D. C. Griffin, *Phys. Rev. A* **72**,052716 (2005).